Halothane and Cyclopiazonic Acid Modulate Ca-ATPase Oligomeric State and Function in Sarcoplasmic Reticulum†

Brad S. Karon, James E. Mahaney, and David D. Thomas*

Department of Biochemistry, University of Minnesota Medical School, Minneapolis, Minnesota 55455

Received April 5, 1994; Revised Manuscript Received August 24, 1994®

ABSTRACT: We have studied the effects of cyclopiazonic acid (CPA) and halothane on the enzymatic activity, oligomeric state, and conformational equilibrium of the Ca-ATPase in skeletal muscle sarcoplasmic reticulum (SR). CPA is a potent inhibitor of Ca-ATPase activity, and this inhibition is competitive with respect to ATP concentration. Time-resolved phosphorescence anisotropy was used to detect the fraction of Ca-ATPase monomers, dimers, and larger aggregates in the absence and presence of CPA. CPA increased the fraction of dimers and larger aggregates of the Ca-ATPase. Addition of halothane to SR, or detergent solubilization of the Ca-ATPase, increased the apparent K_I of CPA inhibition, and increased the fraction of Ca-ATPase present as monomers. CPA stabilized the E2 conformational state of the Ca-ATPase relative to the E1 and E2−P states, as measured by fluorescein 5-isothiocyanate fluorescence and enzyme phosphorylation from inorganic phosphate. E2−P formation in the presence of CPA was partially restored by halothane and solubilization. We conclude that CPA inhibits the Ca-ATPase in part by overstabilizing dimers or small oligomers of the Ca-ATPase, which is correlated with stabilization of the E2 conformation of the enzyme.

The Ca-ATPase of sarcoplasmic reticulum (SR)[1] utilizes ATP to remove calcium from the sarcoplasm in order to relax skeletal muscle. A thoroughly tested and widely accepted model for the enzymatic cycle (Scheme 1) involves two fundamental conformations, E1 and E2, which couple ATP hydrolysis to calcium transport via differences in their affinities and vectorial specificities for ATP and Ca (Inesi, 1985; Froehlich & Heller, 1985; Martonosi et al., 1990). In the absence of substrates, the enzyme exists in equilibrium between E1 and E2 (de Meis, 1988). In the presence of micromolar calcium, the conformational equilibrium shifts strongly toward E1 (Froud & Lee, 1986; Wakabayashi et al., 1990). ATP binds quickly and with high affinity to E1, forming E1·ATP (Dupont, 1980). ATP-dependent formation of the phosphoenzyme (E1−P) is then followed by calcium translocation, which involves a conformational change of the enzyme from a state with high Ca affinity (E1−P) to state with greatly reduced Ca affinity (E2−P) (Froehlich & Heller, 1985). Following Ca translocation, Ca is released from E2−P (Beeler & Keffer, 1984), and E2−P is hydrolyzed to E2 and P_i, completing the enzyme cycle (de Meis, 1988).

Previous investigations into the nature of the E1/E2 transition have suggested that changes in the oligomeric state of the Ca-ATPase may be essential for this conformational transition (Ikemoto et al., 1981a,b). Electron microscopy (EM) of the Ca-ATPase in the presence of vanadate, a phosphate analog that stabilizes the E2 conformation, reveals an orderly pattern of dimeric Ca-ATPase oligomers (Buhle et al., 1983; Taylor et al., 1986). In the presence of Ca or lanthanide ions, which bind with high affinity to the Ca sites associated with the E1 conformation, the Ca-ATPase is seen by EM to form orderly arrays of monomeric units (Dux et al., 1985). These observations led to the proposal that a dimer to monomer transition was essential for the E2 to E1 transition, and thus Ca-ATPase function (Dux et al., 1985). However, other investigators have shown that the Ca-ATPase, detergent-solubilized in a monomeric form, retains its Ca-activated ATPase activity (Moller et al., 1980).

Static EM data are not reliable for studying dynamic changes in the Ca-ATpase oligomeric state essential to enzyme function, and experiments with solubilized Ca-ATPase do not provide information on oligomeric changes that may be necessary for proper coupling of ATP hydrolysis to Ca translocation. Therefore, we have previously used both time-resolved phosphorescence anisotropy and EPR spec-

Scheme 1: Enzymatic Cycle of the Ca-ATPase in SR[a]

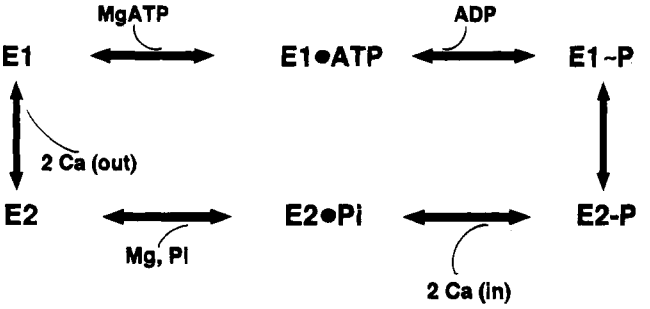

[a] The Ca-ATPase cycles between conformations to pump calcium from the sarcoplasm (outside) into the SR lumen (inside).

† This work was supported by a grant to D.D.T. from the National Institutes of Health (GM27906). J.E.M. was supported by a Grant in Aid from the American Heart Association, Minnesota Affiliate. B.S.K. was supported in part by a predoctoral training grant from NIH.

* To whom correspondence should be addressed.

® Abstract published in *Advance ACS Abstracts,* October 15, 1994.

[1] Abbreviations: SR, sarcoplasmic reticulum; ATP, adenosine 5′-triphosphate; CPA, cyclopiazonic acid; EPR, electron paramagnetic resonance; LSR, light sarcoplasmic reticulum; MOPS, 3-(*N*-morpholino)propanesulfonic acid; NADH, β-nicotinamide adenine dinucleotide, reduced form; DMF, *N,N*-dimethylformamide; ST-EPR, saturation transfer EPR; IASL, iodoacetamide spin-label; ERITC, erythrosin 5-isothiocyanate; FITC, fluorescein 5-isothiocyanate; ERIA, erythrosin 5-iodoacetamide; $C_{12}E_8$, *n*-dodecyl octaethylene glycol monoether.

0006-2960/94/0433-13928$04.50/0

troscopy to obtain a dynamic picture of the SR membrane, correlated with functional studies of the Ca-ATPase (Bigelow & Thomas, 1987; Squier et al., 1988b; Birmachu & Thomas, 1990; Voss et al., 1991; Mahaney et al., 1991; Karon & Thomas, 1993). We have found that agents which increase the average oligomeric size of the Ca-ATPase, such as chemical cross-linkers or the amphipathic peptide melittin, inhibit Ca-ATPase activity (Squier et al., 1988a; Voss et al., 1991; Mahaney et al., 1991). Agents which decrease the average oligomeric size of the Ca-ATPase, such as the volatile anesthetics diethyl ether and halothane, increase Ca-ATPase activity (Bigelow & Thomas, 1987; Birmachu & Thomas, 1990; Karon & Thomas, 1993). These studies suggest that the Ca-ATPase oligomeric state is crucial to proper enzyme function; however, the relationship between oligomeric state, enzyme conformation, and SR function remains unknown.

To investigate this relationship, we have used two different agents to perturb the physical state of the enzyme: cyclopiazonic acid and halothane. Cyclopiazonic acid (CPA) is a specific inhibitor of the Ca-ATPase in SR (Seidler et al., 1989). CPA prevents high-affinity Ca binding to and ATP-dependent phosphorylation of the Ca-ATPase (Goeger & Riley, 1989). CPA also increases the average oligomeric size of the Ca-ATPase (Mersol et al., 1993). Halothane, at clinical levels, increases enzymatic activity and decreases the average oligomeric size of the Ca-ATPase (Karon & Thomas, 1993). At higher levels, halothane inhibits enzymatic activity (Nelson & Sweo, 1988; Louis et al., 1992; Karon & Thomas, 1993), most likely by excessively depleting the number of Ca-ATPase oligomers (Karon & Thomas, 1993). These observations suggest that either overstabilizing Ca-ATPase oligomers (with CPA) or excessively depleting oligomers (with halothane) leads to enzyme inhibition by interfering with essential oligomeric changes necessary for enzyme function. In the present study, we have investigated the physical and functional interactions between CPA and halothane on the Ca-ATPase in SR, in order to gain insight into the relationship between Ca-ATPase oligomeric state, conformational equilibrium, and enzymatic function.

MATERIALS AND METHODS

Reagents and Solutions. Erythrosin 5-isothiocyanate (ERITC), fluorescein 5-isothiocyanate (FITC), and erythrosin 5-iodoacetamide were obtained from Molecular Probes, Inc. (Eugene, OR), and stored in DMF under liquid nitrogen. ATP, CPA, catalase, glucose, and glucose oxidase type IX were obtained from Sigma. Halothane (99%) and spin-labels were obtained from Aldrich, and *n*-dodecyl octaethylene glycol monoether ($C_{12}E_8$) was obtained from CalBiochem (La Jolla, CA). Enzyme-linked activity, phosphorescence anisotropy, and EPR experiments were carried out in a standard buffer containing 60 mM KCl, 50 mM MOPS, 2 mM $MgCl_2$, and 0.1 mM $CaCl_2$, pH 7.0.

Preparations and Assays. Light SR (LSR) vesicles were prepared from the fast twitch skeletal muscle of New Zealand white rabbits (Fernandez et al., 1980). The vesicles were purified on a discontinuous sucrose gradient (Birmachu et al., 1989) to remove heavy and intermediate SR vesicles (junctional SR containing calcium release proteins). All preparation was done at 4 °C. SR pellets were resuspended in 0.3 M sucrose/20 mM MOPS (pH 7.0), rapidly frozen in 4 mg aliquots, and stored in liquid nitrogen until use. LSR consisted of approximately 80% Ca-ATPase, or 7 nmol of Ca-ATPase/mg of SR protein. The ATP hydrolysis of the SR vesicles was fully coupled to calcium transport (Squier & Thomas, 1989). SR lipids were extracted by a modification (Hidalgo et al., 1976) of the method of Folch et al. (1957), using nitrogen-saturated solvents to prevent oxidation. The lipids were stored in chloroform/methanol (2:1) under nitrogen at −20 °C.

SR Ca-ATPase activity was measured at 25 °C using an enzyme-linked, continuous ATPase assay, in the standard buffer with the addition of 5−50 μg/mL SR, 0.42 mM phosphoenolpyruvate, 0.15 mM NADH, 7.5 IU of pyruvate kinase, and 18 IU of lactate dehydrogenase. MgATP was added to start the assay, and the absorbance of NADH was monitored at 340 nm to determine the rate of ATP hydrolysis. All activity measurements (except assays of detergent-solubilized Ca-ATPase) were performed in the presence of 1 μg/mL of the ionophore A23187, which was added to SR prior to the start of the assays. Addition of the ionophore allows the Ca-ATPase activity to be measured in the absence of a Ca gradient, so that any vesicle leakiness produced by the addition of CPA or halothane will not affect the activity measured (Bigelow & Thomas, 1987). The activity measured in the presence of ionophore gives a maximal Ca-ATPase activity, since the enzyme does not have to work against a concentration gradient. Halothane, 30−50% v/v in DMF, was added with a gas-tight Hamilton syringe, by injecting a small amount (less than 1% of the total sample volume) of halothane through a septum in the cuvette. After the addition of CPA and/or halothane, samples were allowed to incubate for 5 min at 25 °C. The volumes of SR and halothane used were adjusted to minimize the vapor space above the SR, so that the amount of halothane that partitioned into the vapor phase was negligible. The final volume of DMF added, up to 1% v/v, did not affect Ca-ATPase activity.

Time-Resolved Phosphorescence Anisotropy. Phosphorescence anisotropy decays were obtained as described previously (Ludescher & Thomas, 1988). The time-dependent phosphorescence anisotropy decay $r(t)$ is given by

$$r(t) = \frac{I_{vv} - GI_{vh}}{I_{vv} + G2I_{vh}} \quad (1)$$

where I_{vv} and I_{vh} are obtained by signal-averaging the time-dependent phosphorescence decays following 2000 laser pulses, with a single detector and a polarizer that alternates between the vertical (I_{vv}) and horizontal (I_{vh}) positions every 2000 pulses. The laser repetition rate was 200 Hz, so a typical $r(t)$ acquisition required 4 min to complete 10 loops, or cycles, or 4000 laser pulses each (2000 in each orientation). G is an instrumental correction factor, determined by measuring the anisotropy of free dye in solution under experimental conditions.

Optical Labeling and Sample Preparation. For phosphorescence experiments, the Ca-ATPase was specifically labeled at lysine-515 with ERITC as described previously (Birmachu & Thomas, 1990). Labeling of the Ca-ATPase with ERIA was accomplished by reacting 0.05 mM Ca-ATPase with 0.1 mM ERIA for 3 h at room temperature (in 25 mM MOPS, 0.3 M sucrose, and 0.1 mM $CaCl_2$, pH 7.0), and then reacting excess dye with BSA as described previously (Birmachu & Thomas, 1990). Oxygen was enzymatically removed from the samples with 200 μg/mL glucose oxidase, 30 μg/mL catalase, and 5 mg/mL glucose,

according to the method of Eads et al. (1984). Deoxygenation was carried out in a sealed cuvette containing 0.2−0.3 mg/mL SR protein for 15−25 min prior to phosphorescence data collection. Halothane, 30−50% v/v in DMF, was added to the SR in a manner analogous to the technique used for activity measurements. The final concentration of DMF, up to 0.5% v/v, did not affect the anisotropy decay of SR. Samples were incubated 5−15 min at room temperature after the addition of CPA and/or halothane. For fluorescence experiments, the Ca-ATPase was specifically labeled with FITC using the same procedure as for ERITC labeling (Birmachu & Thomas, 1990). The fluorescence intensity of 0.5 μM FITC-LSR was measured with a SPEX Fluorolog II fluorometer (λ_{ex} = 495 nm, λ_{em} = 520 nm) by summing the total fluorescence emission over 20 s. This was repeated 4 times/sample, and the average represents the intensity value for one experiment. The experiments were performed in the standard buffer (high calcium) or a buffer containing 60 mM KCl, 50 mM MOPS, 2 mM $MgCl_2$, and 1 mM EGTA, pH 7.0 (low calcium).

Data Analysis. Phosphorescence anisotropy decays were analyzed as reported previously (Birmachu & Thomas, 1990), using a nonlinear least-squares fit to a sum of exponentials plus a constant:

$$r(t)/r_0 = \sum_{i=1}^{n} A_i \exp(-t/\phi_i) + A_\infty \qquad (2)$$

where ϕ_i are rotational correlation times, A_i are the normalized amplitudes (r_i/r_0), A_∞ is the normalized residual anisotropy (r_∞/r_0), and r_0 is the initial anisotropy [$r(0) = r_0 - \sum_{r_i} + r_\infty$]. The goodness-of-fit for the anisotropy decays was evaluated by comparing χ^2 values for the multiexponential fits, and by comparing plots of the residuals (the difference between the measured and the calculated decays). Phosphorescence lifetimes were determined by fitting the total intensity ($I_{vv} + 2I_{vh}$) to a sum of exponentials in a manner analogous to the anisotropy decay fitting (Birmachu & Thomas, 1990). Halothane and CPA, at the concentrations used in the experiments, did not have significant effects on phosphorescence lifetimes. At higher concentrations, however, both agents quenched the phosphorescence of ERITC-labeled SR.

It has been shown previously (Birmachu & Thomas, 1990) that the phosphorescence anisotropy decay of ERITC-SR is dominated by the uniaxial rotation of the labeled Ca-ATPase about an axis normal to the bilayer. For this model, each different rotational diffusion coefficient should give rise to a biexponential decay component [Kinosita et al., 1984; reviewed by Thomas (1986)], but it has been shown that a single-exponential approximation is sufficient to describe the decay for each rotating species in ERITC-SR (Birmachu & Thomas, 1990). As long as the probe orientation relative to the protein is the same for all proteins, anisotropy decay amplitudes (A_i, eq 2) will be proportional to the mole fraction (f_i) of protein having a rotational correlation time ϕ_i:

$$A_i \propto f_i \qquad A_\infty' \propto f_I \qquad (3)$$

where f_I is the mole fraction of probes (i.e., proteins) that are immobile on the time scale of the experiment (Birmachu et al., 1993), and $A_\infty' = A_\infty - A_{\infty 0}$. $A_{\infty 0}$ is the residual anisotropy of a sample with no immobile Ca-ATPase aggregates ($f_I = 0$, i.e., control LSR at 25 °C) and describes the extent to which the probe's motion is restricted in angular range, due to the fixed angles θ_a and θ_e of the probe's absorption (μ_a) and emission (μ_e) transition moments relative to the membrane normal.

The Saffman−Delbrück equation describes the rotational diffusion coefficient (rotational mobility) for uniaxial rotation of a cylindrical membrane protein expressed as a function of the membrane lipid viscosity (η), temperature (T), and the effective radius (a) of the portion of the protein in the bilayer (Saffman & Delbrück, 1975):

$$D_m = kT/4\pi a^2 h\eta \qquad (4)$$

where h is the thickness of the hydrocarbon phase of the lipid bilayer. Thus, the rotational mobility ($1/\phi$, the reciprocal of the rotational correlation time) should be proportional to the lipid fluidity (T/η; Squier et al., 1988b) and inversely proportional to the intramembrane area ($\pi a^2 h$) of the rotating protein. Therefore, increasing lipid fluidity or decreasing protein size (formation of smaller oligomers) should result in increased rotational mobility. This theory relating protein size and lipid fluidity to protein rotational mobility is supported by previous studies on the Ca-ATPase, as measured by either ST-EPR (Squier et al., 1988a,b) or phosphorescence anisotropy (Birmachu & Thomas, 1990). Using this theory, Birmachu and Thomas (1990) showed that correlation times (ϕ_i) obtained by fitting anisotropy decays can be used to determine the sizes of Ca-ATPase oligomers, and normalized amplitudes (A_i) can be used to determine the fraction of the different oligomers present in SR.

Spin-Labeling and Sample Preparation. SR bilayer hydrocarbon chain rotational mobility was measured using a stearic acid derivative containing the spin-label at the C-5 position (5-SASL), incorporated into protein-free aqueous dispersions of SR lipids. Incorporation of 5-SASL into SR lipid was accomplished by adding the spin-label to extracted lipids in a chloroform/methanol (2:1 v/v) mixture prior to drying with nitrogen. The spin-labeled lipid was lyophilized overnight, and then resuspended in the standard buffer to a concentration of 40−50 mM.

EPR Spectroscopy. EPR spectra were acquired using a Bruker ESP-300 spectrometer equipped with a Bruker ER4102 cavity, and digitized with the spectrometer's built-in microcomputer using Bruker OS-9-compatible ESP 1620 spectral acquisition software. Spectra were downloaded to an IBM-compatible microcomputer and analyzed using software developed in our laboratory by R. L. H. Bennett. Conventional (V_1) EPR was used to detect submicrosecond motions of the lipid spin-labels. V_1 spectra were obtained using 100 kHz field modulation (with a peak-to-peak modulation amplitude of 2 G), with microwave field intensities (H_1) of 0.14 G. Sample temperature was controlled to within 0.5 °C with a Bruker ER 4111 variable-temperature controller, and monitored with a Sensortek Bat-21 digital thermometer using an IT-21 thermocouple probe inserted into the top of the sample capillary, so that it did not interfere with spectral acquisition.

EPR Spectral Analysis. Fatty acid spin-label spectra were analyzed by measuring the inner ($2T_\perp'$) and outer ($2T_{||}'$) spectral splittings [see Mahaney and Thomas (1991)]. The effective order parameter (S) was calculated from the spectral splittings according to Gaffney (1976):

$$S = \frac{T'_{\parallel} - (T'_{\perp} + C)}{T'_{\parallel} + 2(T'_{\perp} + C)} 1.66 \quad (5)$$

where $C = 1.4 - 0.053\ (T'_{\parallel} - T'_{\perp})$.

Ca Loading of SR Vesicles. SR vesicles were Ca loaded by incubating the ERITC-labeled SR in a buffer containing 50 mM MOPS, 10 mM $CaCl_2$, and 10 mM $MgSO_4$, pH 6.5, on ice for at least 4 h. To start phosphorescence anisotropy experiments, 125 μL of control (not Ca-loaded) or Ca-loaded SR was added to 4.5 mL of buffer containing 50 mM MOPS, 60 mM KCl, 2 mM $MgCl_2$, and 1 mM EGTA, pH 6.5, at 4 °C in the presence of deoxygenating enzymes in a sealed cuvette. Phosphorescence anisotropy experiments were performed at 4 °C because we have observed that the efflux of Ca from Ca-loaded IASL-labeled SR vesicles proceeds slowly at 4 °C, with nearly 80% of the Ca remaining in the vesicles after 30 min (data not shown). Phosphorescence anisotropy experiments at 4 °C were completed within 20 min of introducing the Ca-loaded SR to the Ca-free environment; thus, little Ca loss from SR vesicles was anticipated during the anisotropy experiments.

Enzyme Phosphorylation from Inorganic Phosphate. Prior to phosphorylation, SR vesicles (0.5 mg/mL) or $C_{12}E_8$-solubilized Ca-ATPase (0.5 mg/mL) was suspended in a buffer containing 10 mM $MgCl_2$, 2 mM EGTA, and 100 mM MOPS, pH 6.5. During the experiments involving halothane, halothane and/or CPA was incubated at room temperature with SR in the same buffer in a sealed vial for 5 min; then SR was transferred to another sealed vial for the phosphorylation reaction. For experiments involving only CPA, CPA was incubated at room temperature with SR or $C_{12}E_8$-solubilized Ca-ATPase for 5 min prior to the phosphorylation reaction or after the reaction had reached equilibrium. To initiate the phosphorylation reaction, an equal volume of 8 mM $Na_2H^{32}PO_4$ in the same buffer was added to the samples and vortexed. At the indicated time, the reaction was quenched by the addition of 3% perchloric acid + 2 mM H_3PO_4 (final concentrations). The quenched samples were pelleted in a tabletop centrifuge and then washed 3 times with a solution of 5% trichloroacetic acid, 4 mM H_3PO_4, 6 mM polyphosphate, and 5 mM cold ATP. The final pellets were dissolved in 2 mL of 1 N NaOH overnight, and the ^{32}P-phosphoenzyme was assayed by counting the Cerenkov radiation.

RESULTS

Effects of CPA and Halothane on Ca-ATPase Activity. Ca-ATPase activity was measured in order to determine the effects of CPA and halothane on Ca-ATPase function. CPA inhibited Ca-ATPase activity, with complete inhibition of Ca-ATPase activity occurring by 1 μM total added CPA, or approximately 20 mol of CPA/mol of ATPase. High levels of halothane (7.6 mM) inhibited the Ca-ATPase in the absence of CPA, as observed previously (Karon & Thomas, 1993). Halothane partially protected the Ca-ATPase from CPA inhibition when it was added to SR in the presence of CPA. Under these conditions (CPA + 7.6 mM halothane), the activity of the Ca-ATPase was higher than that observed in the presence of CPA alone (Figure 1). Halothane had no protective effect on Ca-ATPase activity in the presence of the ATPase inhibitors thapsigargin (a plant toxin) and melittin (an amphipathic peptide from bee venom) (data not shown).

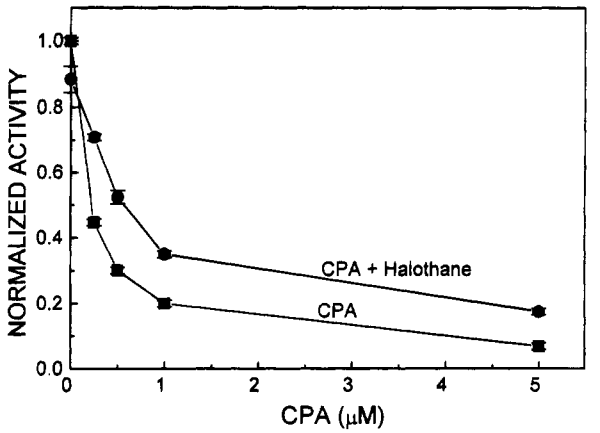

FIGURE 1: Normalized Ca-ATPase activity (normalized to the activity of SR with no added CPA or halothane) determined by an enzyme-linked ATPase assay at 25 °C, as described under Materials and Methods. Assays were performed in the presence of 2 mM ATP and in the absence (CPA) or presence (CPA + halothane) of 7.6 mM halothane. Values represent the average of four experiments ± the standard error of the mean.

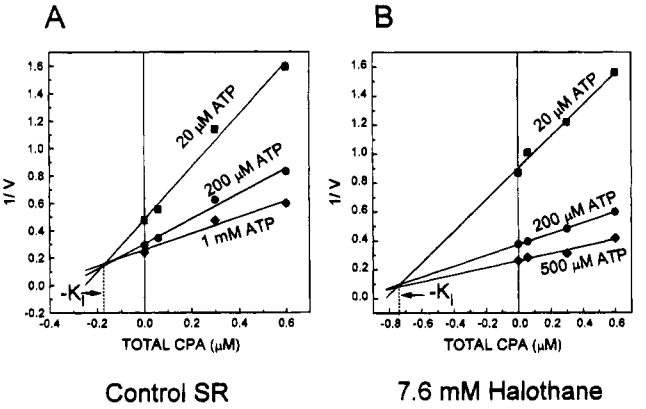

FIGURE 2: Dixon plots ($1/V = 1/\text{activity}_{TU}$) showing CPA competitive inhibition of the Ca-ATPase. The abscissa gives the total concentration of CPA added. Enzyme-linked ATPase assays were performed at 25 °C as described under Materials and Methods, and each point represents the average of three experiments. The lines are the best fit (by least-squares analysis) to the data at each ATP concentration, and the apparent K_I is determined by averaging the intersections of the three lines ± the standard deviation. In panel A, CPA inhibition of control SR (no halothane) is shown at 20 μM (■), 200 μM (●), and 1 mM (♦) ATP. In panel B, CPA inhibition of SR in the presence of 7.6 mM halothane is shown at 20 μM (■), 200 μM (●), and 500 μM (♦) ATP.

Seidler et al. (1989) previously observed that CPA inhibition of the Ca-ATPase was competitive with respect to ATP concentration. To further define this effect, we measured the inhibitory effects of CPA at several [ATP] either alone or in the presence of 7.6 mM halothane. We observed that CPA inhibition was competitive with respect to ATP concentration, and we obtained an apparent K_I of 162 ± 18 nM (Figure 2, panel A). In the presence of 7.6 mM halothane, CPA inhibition was also competitive with respect to [ATP], but the apparent K_I increased to 782 ± 52 nM, 4.8 times as large as the K_I in the absence of halothane (Figure 2, panel B). Because it was not possible to measure CPA binding to the Ca-ATPase, the apparent K_I represents an upper limit for the binding of CPA to the enzyme, rather than an actual binding constant.

The primary physical effect of halothane on LSR at 25 °C is to decrease the extent of ATPase−ATPase interactions (decrease the average oligomeric size) (Karon & Thomas, 1993). To determine whether Ca-ATPase dissociation alone

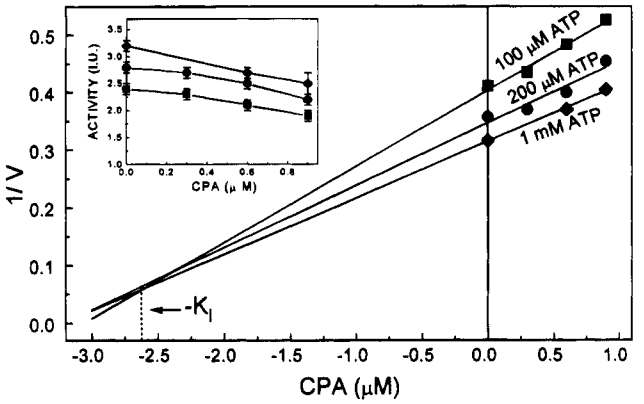

FIGURE 3: Dixon plot ($1/V$ = 1/activity$_{IU}$) showing CPA competitive inhibition of $C_{12}E_8$-solubilized Ca-ATPase at 100 μM (■), 200 μM (●), and 1 mM (♦) ATP. The abscissa gives the total concentration of CPA added. Enzyme-linked assays were performed at 25 °C as described under Materials and Methods, and each point represents the average of three experiments. The lines are the best fit (by least-squares analysis) to the data at each ATP concentration, and the K_I is determined by averaging the intersections of the three lines ± the standard deviation. The inset is a plot of activity (IU) vs [CPA] (μM) for the same data, showing that inhibition is not complete by 1 μM CPA.

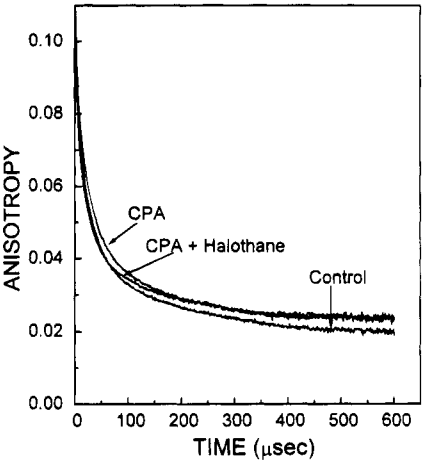

FIGURE 4: Time-resolved phosphorescence anisotropy decays of ERITC-labeled LSR at 25 °C in standard buffer in the absence (control) and presence of 20 μM CPA (CPA) or 20 μM CPA + 7.6 mM halothane (CPA + halothane).

could protect against CPA inhibition, we used the detergent $C_{12}E_8$ to solubilize the Ca-ATPase under conditions that stabilize 70−80% of the Ca-ATPase in the monomeric state (Mollier et al., 1980). $C_{12}E_8$-solubilized Ca-ATPase differed from native SR in the [ATP] dependence of Ca-ATPase activity. Compared to Ca-ATPase in native SR, the activity of solubilized Ca-ATPase showed much less [ATP] dependence between 100 μM and 1 mM ATP, and ***no*** [ATP] dependence between 5 and 100 μM ATP, in agreement with a previous study (Moller et al., 1980). Furthermore, ATP was not competitive with respect to CPA inhibition of Ca-ATPase activity below 100 μM ATP (not shown). $C_{12}E_8$, added to SR prior to the addition of CPA, further protected the Ca-ATPase from the inhibitory effects of CPA. The apparent K_I of CPA for $C_{12}E_8$ solubilized Ca-ATPase increased to 2730 ± 350 nM, 17 times as large as the K_I in the absence of $C_{12}E_8$ (Figure 3). In addition, CPA inhibition of solubilized Ca-ATPase was not complete by 1 μM CPA (Figure 3, inset), as was the case for native SR (Figure 1).

Effect of CPA on SR Lipid Fluidity. We used EPR spectroscoopy to determine the effect of CPA on SR bilayer fluidity using protein-free, aqueous dispersions of extracted SR lipids. The lipid dispersions were spin-labeled with a stearic acid derivative labeled at the 5-carbon position, which is sensitive to bilayer fluidity near the headgroup of the bilayer (Mahaney & Thomas, 1991). CPA, at 385 μM, had no effect on the order parameters measured from EPR spectral splittings, indicating that CPA does not affect the SR bilayer fluidity (Squier et al., 1988b).

Effects of CPA and Halothane on the Rotational Dynamics of the Ca-ATPase. Time-resolved phosphorescence anisotropy experiments were performed to determine the effects of CPA, and CPA + halothane, on the rotational dynamics of the Ca-ATPase in SR. Figure 4 shows the anisotropy decays of ERITC-LSR in the presence of either 20 μM CPA (10:1 CPA:ATPase ratio) or 20 μM CPA + 7.6 mM halothane. Addition of CPA results in a less rapid anisotropy decay, and a higher residual anisotropy ($A_\infty' \neq 0$, eq 3). Similar effects were observed when 7.6 mM halothane was added after the addition of either 10 μM or 40 μM CPA.

Table 1: Anisotropy Decay Parameters for ERITC-LSR at 25 °C[a]

sample	r_0	A_1	ϕ_1	A_2	ϕ_2	A_3	ϕ_3	A_∞'
control	0.11	0.23	5 ± 1	0.41	28 ± 1	0.20	209 ± 7	0.00
20 μM CPA	0.11	0.14	5 ± 1	0.46	28 ± 1	0.21	209 ± 7	0.03
CPA + Hal	0.11	0.24	5 ± 1	0.34	23 ± 1	0.20	158 ± 18	0.04

[a] Time-resolved phosphorescence anisotropy parameters were determined by fitting the anisotropy decays of ERITC-LSR at 25 °C in the absence or presence of 20 μM CPA or 20 μM CPA + 7.6 mM halothane (CPA + Hal), as described under Materials and Methods. The correlation times (ϕ_i, microseconds) represent the average of four experiments ± the standard error of the mean (SEM). The SEM for all r_0, A_i, and A_∞' values is 0.01 (n = 4).

To quantify the effects of CPA, and CPA + halothane, on the rotational dynamics of the Ca-ATPase, we fit the anisotropy decays as described under Materials and Methods (eq 2). The correlation times (ϕ_i) reflect the rotational mobility of the Ca-ATPase (related to lipid fluidity, T/η, eq 4), while the amplitudes (A_i) are proportional to the fraction of Ca-ATPase with a given rotational mobility (i.e., the fraction of Ca-ATPase in a given oligomeric state, eq 3). The decays were best fit to a sum of three exponentials plus a residual anisotropy, as observed previously (Birmachu & Thomas, 1990; Karon & Thomas, 1993). Although it is not possible to make a precise assignment of amplitudes to oligomeric states, the three components are interpreted to represent the rotational mobility of the smallest Ca-ATPase units (most likely monomers, A_1), small oligomers (perhaps dimers, A_2), and larger aggregates (A_3), as discussed previously (Birmachu & Thomas, 1990; Karon & Thomas, 1993). The fraction of the largest Ca-ATPase aggregates, not rotating on the time scale of the TPA experiment (600 μs), is represented by A_∞' (eq 3). Because CPA does not affect the fluidity of SR lipids (as detected by EPR), the correlation times were fixed to the control values (no CPA or halothane) in fitting the anisotropy decays taken in the presence of CPA alone. The correlation times (ϕ_i), amplitudes (A_i), r_0, and A_∞' values for the control, CPA, and CPA + halothane samples are given in Table 1. CPA addition decreased the value of A_1 by 39% (from 0.23 to 0.14), while increasing the values of A_2 and A_∞'. These changes are consistent with a change in the equilibrium between monomers and small oligomers to favor small oligomers, as well as an increase in the fraction of immobilized Ca-ATPase (Karon & Thomas, 1993). Halothane addition following CPA increased the

Table 2: Fluorescence Intensity of FITC-LSR at 25 °C[a]

FITC-LSR sample ($[Ca]_{free}$)	intensity/10^7	ΔF(corr)
100 μM Ca (100 μM)	3.27 ± 0.01	
100 μM Ca + 0.5 mM EGTA (100 nM)	3.45 ± 0.01	8
100 μM Ca (100 μM)	3.30 ± 0.01	
100 μM Ca + 5 μM CPA (100 μM)	3.23 ± 0.01	0
Ca, CPA, + 0.5 mM EGTA (100 nM)	3.78 ± 0.01	18
1 mM EGTA (0)	3.59 ± 0.01	
1 mM EGTA + 1 mM Ca (20 μM)	3.26 ± 0.01	−7
1 mM EGTA (0)	3.61 ± 0.04	
1 mM EGTA + 5 μM CPA (0)	3.90 ± 0.04	10
EGTA, CPA, + 1 mM Ca (20 μM)	3.70 ± 0.06	5

[a] Intensity of FITC-LSR fluorescence measured as described under Materials and Methods. The samples were prepared in a buffer containing either 100 μM Ca or 1 mM EGTA, and the free calcium concentration (given in parentheses after each sample) was calculated as described previously (Voss et al., 1994). The total intensity represents the average of four experiments ± the standard error of the mean. ΔF(corr) is the percent change $[(F - F_0)/F_0]$ from control (either 100 μM Ca or 1 mM EGTA) corrected for the effects of sample dilution, which was calculated by adding an equal volume of water to the sample under experimental conditions.

value of A_1 by 71% (from 0.14 to 0.24) and decreased the value of A_2, but did not affect A_∞'. This is consistent with the dissociating effects of halothane observed previously, except it is apparent that halothane cannot dissociate the largest (immobile) Ca-ATPase aggregates induced by CPA.

Effects of CPA on the Fluorescence of FITC-LSR. The fluorescence intensity of the bound form of FITC, a fluorescent probe similar in structure of ERITC, is sensitive to conformational changes of the Ca-ATPase between E1 and E2 (Froud & Lee, 1986; Sagara et al., 1992). Because previous studies have suggested that CPA interacts with an E2-like form of the Ca-ATPase (Goeger & Riley, 1989; Seidler et al., 1989), we investigated the effect of CPA on the fluorescence of FITC-LSR (Table 2). We found that addition of 0.5 mM EGTA to FITC-LSR in the presence of 100 μM Ca (change in free [Ca] from 100 μM to 100 nM) increased FITC fluorescence by 8%. Addition of 1 mM Ca to FITC-LSR in the presence of 1 mM EGTA (change in free [Ca] from 0 to 20 μM) decreased FITC fluorescence by 7%. These results are consistent with previous studies finding that addition of EGTA to FITC-SR in the presence of Ca increases intensity (indicating a change in conformation from E1 to E2), while addition of Ca to FITC-SR in the presence of EGTA decreases fluorescence intensity (indicating a change in conformation from E2 to E1) (Froud & Lee, 1986; Sagara et al., 1992). CPA did not affect the intensity of FITC-LSR in the presence of 100 μM Ca (>99% E1 conformation; Alonso & Hecht, 1990), and addition of EGTA following CPA resulted in a greater increase in fluorescence intensity than addition of EGTA alone (Table 2). CPA increased the intensity of fluorescence when added in the presence of 1 mM EGTA (favoring E2 conformation), and subsequent addition of 1 mM calcium did not decrease fluorescence intensity beyond control levels (EGTA alone, Table 2). These results demonstrate that CPA does not interact with the E1 conformation of the Ca-ATPase, but preferentially interacts with the E2 conformation, stabilizing that form of the enzyme and preventing the E2 to E1 transition.

Effects of CPA, Halothane, and $C_{12}E_8$ on Phosphorylation by P_i. Because our experiments with FITC-LSR indicated that CPA was interacting with the E2 conformation of the

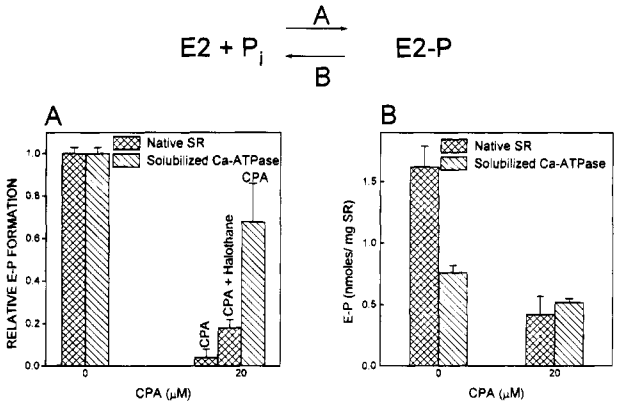

FIGURE 5: Panel A: Relative steady-state Ca-ATPase phosphorylation by inorganic phosphate (E−P formation) at very low [Ca] (2 mM EGTA, no added Ca) in the absence and presence of 20 μM CPA, 20 μM CPA + 7.6 mM halothane, or 20 μM CPA added to $C_{12}E_8$-solubilized Ca-ATPase (normalized to the level of E−P formed by solubilized Ca-ATPase in the absence of CPA). CPA was added and allowed to incubate for 5 min; then SR or solubilized Ca-ATPase was incubated with $Na_2H^{32}PO_4$ in the absence or presence of CPA for 5 min at room temperature. The reaction was then quenched, and E−P levels were determined as described under Materials and Methods. Values represent the average of 2−5 experiments ± the standard deviation. Panel B: Effect of [CPA] on steady-state levels of E−P. $Na_2H^{32}PO_4$ was added to SR or solubilized Ca-ATPase and incubated at room temperature for 5 min to reach equilibrium; then 20 μM CPA was added and allowed to incubate for an additional 5 min before the reaction was quenched and E−P levels determined. Values represent the average of four experiments ± the standard deviation.

Ca-ATPase, we investigated whether CPA affects the phosphorylation of the enzyme from inorganic phosphate at very low calcium (2 mM EGTA, no added Ca). Under these conditions, the enzyme is stabilized in the E2 conformation (Scheme 1), and the Ca-ATPase can be phosphorylated by inorganic phosphate to form E2−P (deMeis, 1988). CPA strongly inhibited the extent of steady-state phosphorylation of E2 by inorganic phosphate. Halothane (7.6 mM), and $C_{12}E_8$ solubilization of the Ca-ATPase, partially protected the Ca-ATPase from CPA inhibition of E2 phosphorylation (Figure 5, panel A). Addition of 20 μM CPA reduced steady-state E−P levels to 4 ± 4% of the control (no CPA), while 7.6 mM halothane increased E−P levels to 18 ± 4% of the control, or 4.5 times (18%/4% = 4.5) the E−P obtained in the presence of CPA alone. The level of E−P formed by $C_{12}E_8$-solubilized Ca-ATPase in the presence of 20 μM CPA was 68 ± 18% of the level formed by control $C_{12}E_8$-solubilized enzyme (no CPA). This E−P level was 17 times (68%/4% = 17) the relative level reached in the presence of CPA alone (CPA-treated native SR) (Figure 5, panel A). CPA also reduced the amount of E2−P remaining when the inhibitor was added *after* steady-state levels of E2−P had been reached. $C_{12}E_8$ solubilization of the Ca-ATPase reduced but did not eliminate the effects of CPA on steady-state levels of E2−P (Figure 5, panel B).

Effects of Ca Loading on the Rotational Dynamics of the Ca-ATPase. It has previously been shown that loading of SR vesicles with millimolar concentrations of intravesicular calcium inhibits Ca-ATPase activity (de Meis & Sorenson, 1989). In addition, the rate of phosphorylation of the Ca-ATPase from inorganic phosphate is slower in this "back-inhibited" SR than in control (low intravesicular Ca) SR, suggesting that Ca loading of SR vesicles stabilizes the E2 state of the Ca-ATPase relative to the E2−P state (Chaloub et al., 1979). Since the results of our steady-state phos-

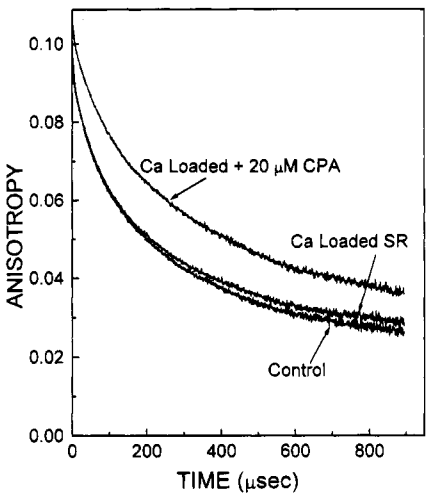

FIGURE 6: Time-resolved phosphorescence anisotropy decays of ERITC-labeled LSR at 4 °C in the absence (control) and presence (Ca-loaded SR) of 10 mM intravesicular Ca, and in the presence of 10 mM intravesicular Ca + 20 μM CPA (Ca-loaded + 20 μM CPA).

Table 3: Anisotropy Decay Parameters for ERITC-LSR at 4 °C[a]

sample	r_0	A_1	ϕ_1	A_2	ϕ_2	A_3	ϕ_3	A_∞'
control	0.10	0.09	5 ± 1	0.20	54 ± 1	0.48	315 ± 7	0.05
20 μM CPA	0.11	0.08	5 ± 1	0.13	54 ± 1	0.54	315 ± 7	0.07
Ca loaded	0.10	0.10	5 ± 1	0.20	57 ± 1	0.45	311 ± 6	0.08
Ca loaded + CPA	0.11	0.09	5 ± 1	0.10	57 ± 1	0.50	311 ± 6	0.13

[a] Time-resolved phosphorescence anisotropy decay parameters were determined by fitting the anisotropy decays of ERITC-LSR at 4 °C in the absence or presence of 20 μM CPA (control and 20 μM CPA), and in the presence of 10 mM intravesicular Ca ± 20 μM CPA (Ca loaded and Ca loaded + CPA), as described under Materials and Methods. The correlation times (ϕ_i, microseconds) represent the average of three experiments ± the standard error of the mean (SEM). The SEM for all r_0, A_i, and A_∞' values is 0.01 (n = 3).

phorylation experiments suggest that CPA stabilizes the E2 conformation of the Ca-ATPase relative to the E2−P state, and anisotropy experiments indicate that CPA increases the average oligomeric size of the enzyme, we determined the effects of Ca loading SR vesicles on the oligomeric state of the Ca-ATPase. Figure 6 shows the anisotropy decays of control and Ca-loaded ERITC-LSR at 4 °C, and the correlation times (ϕ_i), amplitudes (A_i), r_0, and A_∞' values for control, Ca-loaded, control + CPA, and Ca-loaded + CPA samples are given in Table 3. Ca-loaded SR contains a slightly higher fraction of immobile Ca-ATPase (A_∞') than control (not Ca loaded) SR (Figure 6), and Ca loading sensitizes the Ca-ATPase toward CPA-induced aggregation. In the control SR (not Ca loaded, 4 °C), addition of 20 μM CPA results in more large (A_3) aggregates being formed, with an increase in the fraction of immobile (A_∞') aggregates (Table 3). CPA addition to Ca-loaded SR results in an increase in large (A_3) aggregates, and an even greater (compared to the effect of CPA on the control) increase in the fraction of immobile aggregates.

In order to determine whether changes in Ca-ATPase conformation, rather than oligomeric state, might explain differences in anisotropy decays induced by Ca loading of SR vesicles or CPA, we compared the fluorescence intensity of FITC-LSR to ERITC-LSR. The fluorescence intensity of ERITC-LSR was independent of Ca concentration, indicating that ERITC-LSR fluorescence is not sensitive to Ca-ATPase conformation. In addition, phosphorescence

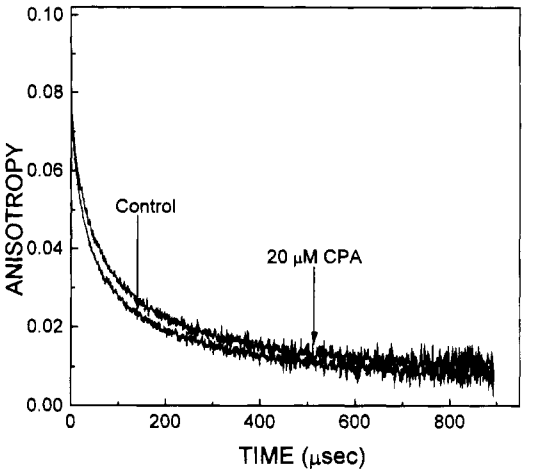

FIGURE 7: Time-resolved phosphorescence anisotropy decays of ERIA-labeled LSR in standard buffer at 25 °C in the absence (control) and presence of 20 μM CPA.

intensity and lifetimes were independent of Ca concentration (between 0 and 100 μM Ca), and phosphorescence anisotropy decays of ERITC-LSR in the presence of 1 mM EGTA, pH 6.5 (strongly favoring the E2 conformation), or 100 μM Ca, pH 7.0 (strongly favoring the E1 conformation), were nearly identical. Thus, changes in the anisotropy decays of ERITC-LSR induced by Ca loading of SR vesicles and CPA do not reflect changes in Ca-ATPase conformation, but rather changes in Ca-ATPase oligomeric state.

It has previously been determined that the anisotropy decay of ERITC-labeled Ca-ATPase in skeletal SR is due to the uniaxial diffusion of the Ca-ATPase in SR, rather than other probe or protein motions such as Ca-ATPase segmental motion (Birmachu & Thomas, 1990). To further verify this finding, we labeled the Ca-ATPase with erythrosin 5-iodoacetamide (ERIA). Iodoacetamide labels have been shown to bind specifically to cysteine-674 on the Ca-ATPase, 56−68 Å away from the binding site for FITC (and thus ERITC) (Bishop et al., 1988). Thus, segmental motion of the Ca-ATPase resulting in a decay in the anisotropy observed with the ERITC label should not be similar to segmental motion detected with the ERIA label. Though the extent and specificity of labeling were not quantitated, phosphorescence anisotropy decays were obtained after labeling of LSR with ERIA as described under Materials and Methods (Figure 7). The initial (r_0) and residual (r_∞) anisotropy of ERIA-labeled LSR appears lower than that observed for ERITC-labeled LSR, which may be due to different angles between the membrane normal and the two probes' emission and excitation dipoles (eq 3). However, the anisotropy decays of ERIA-LSR in the presence and absence of CPA are qualitatively similar to the ERITC-labeled samples (compare Figures 4 and 7). These experiments provide further evidence that the anisotropy decay observed for ERITC-labeled SR is due to the uniaxial diffusion of the Ca-ATPase in SR, rather than ATPase segmental motion. Further investigation is needed to determine the extent and specificity of ERIA labeling, and to quantitatively compare the anisotropy decays of ERITC-labeled and ERIA-labeled Ca-ATPase.

DISCUSSION

Effects of CPA on Ca-ATPase Activity. We have found that CPA inhibits Ca-ATPase activity with nanomolar

affinity, and that this inhibition is competitive with respect to ATP concentration, in agreement with a previous study (Seidler et al., 1989). We have determined an apparent K_I of 162 ± 18 nM for CPA inhibition of Ca-ATPase activity (Figure 2, panel A). Addition of 7.6 mM halothane to SR immediately after CPA resulted in an apparent K_I of 782 ± 52 nM (Figure 2, panel B), 4.8 times as high as the value measured in the absence of halothane. Because it was not possible to measure CPA binding to the Ca-ATPase, the apparent K_I represents an upper limit for the binding of CPA to the Ca-ATPase, rather than an actual binding constant.

There are three possible explanations for the effect of halothane on CPA inhibition: either (a) halothane reacts chemically with CPA, diminishing CPA efficacy for ATPase inhibition, (b) halothane interferes with CPA binding to the Ca-ATPase, or (c) halothane does not interfere with CPA binding to the ATPase, but induces some physical change in SR that reduces the efficacy of CPA for ATPase inhibition. It is unlikely that halothane reacts chemically with CPA, because halothane is an extremely inert chemical, a property essential to volatile anesthetics (Stephen & Little, 1961). Therefore, we will consider the physical effects of CPA and halothane on the Ca-ATPase and the SR membrane.

Effects of CPA and Halothane on the Oligomeric State of the Ca-ATPase. The analysis of previous phosphorescence anisotropy studies has been complicated by the ambiguity in assigning specific decay amplitudes to Ca-ATPase oligomeric states (Birmachu & Thomas, 1990; Karon & Thomas, 1993). Electron microscopy of SR indicates that the Ca-ATPase *in situ* consists predominantly of monomers and small oligomers, with some tetramers (Franzini-Armstrong & Ferguson, 1985). In our previous study, we determined that the primary action of halothane on SR is to dissociate Ca-ATPase oligomers (Karon & Thomas, 1993). In the present study, we have found that addition of CPA to SR at 25 °C results in a slower anisotropy decay, reflected by a decrease in the value of A_1, an increase in A_2, and little change in A_3 or A_∞'. Addition of halothane (7.6 mM) following CPA increased A_1 and decreased A_2.

If the increase in the value of A_1 induced by halothane is due to an increased fraction of Ca-ATPase monomers, then other perturbants that stabilize Ca-ATPase monomers should also have a protective effect against CPA inhibition. $C_{12}E_8$ solubilization of the Ca-ATPase, which stabilizes 70−80% of the enzyme in the monomeric state (monomerizes the Ca-ATPase to a greater extent than halothane addition), resulted in a 17-fold increase in the apparent K_I of CPA inhibition, compared to a 4.8-fold increase in the apparent K_I induced by halothane. Thus, our phosphorescence anisotropy results in the presence of CPA and halothane suggest that an increase in A_1 indicates an increase in the fraction of Ca-ATPase monomers present, while a decrease in A_2 indicates a decrease in the fraction of Ca-ATPase dimers or small oligomers in SR (which dissociate to form monomers).

CPA addition resulted in an approximately 90% inhibition of Ca-ATPase activity (Figure 1), while the value of A_1 was decreased only 39% by CPA. When the Ca-ATPase is solubilized in a monomeric form, CPA inhibition of the Ca-ATPase is reduced but not eliminated (Figure 3). Halothane addition to SR in the presence of CPA increased Ca-ATPase activity an average of 66% compared to the activity measured in the presence of CPA alone (Figure 1). This same level of halothane resulted in a 71% increase (relative to CPA alone) in the value of A_1. It is apparent that changes in the Ca-ATPase oligomeric state alone cannot explain CPA-induced inhibition of the Ca-ATPase, though halothane protection against CPA-induced inhibition correlates well with halothane-induced changes in Ca-ATPase oligomeric state. Thus, we conclude that CPA-induced inhibition of enzymatic activity is in part dependent upon the oligomeric state of the Ca-ATPase.

CPA also increased the fraction of immobile Ca-ATPase aggregates (A_∞'), and this effect was not reversed by halothane. We have previously observed that the oligomeric state of the Ca-ATPase has profound effects on the activity of the enzyme, such that increases in the fraction of immobile aggregates correlate with enzyme inhibition (Squier et al., 1988a; Voss et al., 1991). The role that these large aggregates play in the mechanism of enzyme inhibition is not well understood, as previous studies have shown that under physiological conditions the Ca-ATPase exists predominantly as monomers and small oligomers (Birmachu et al., 1990; Franzini-Armstrong & Ferguson, 1985). Because CPA-induced changes in the fraction of monomers and small oligomers at 25 °C are reversible, whereas CPA-induced changes in the fraction of immobile aggregates are not, it is possible that the large-scale aggregation of the Ca-ATPase induced by inhibitors reflects further aggregation of ATPase dimers or small oligomers that follows inhibition of the Ca-ATPase in the dimer form. This pattern of aggregation may be similar to vanadate-induced crystallization of the Ca-ATPase, in which vanadate-inactivated ATPase dimers form highly organized crystal lattices (Buhle et al., 1983).

Effect of $C_{12}E_8$ Solubilization on CPA Inhibition of the Ca-ATPase. We have proposed two mechanisms by which halothane may protect the Ca-ATPase from CPA inhibition: either halothane (a) interferes with CPA binding to the Ca-ATPase or halothane (b) induces some physical change in SR that reduces the efficacy of CAP for Ca-ATPase inhibition. The effects of CPA on $C_{12}E_8$-solubilized Ca-ATPase help distinguish between the two mechanisms, if we first consider the regulation of native and solubilized Ca-ATPase by ATP in the absence of CPA. In native SR, it has been established that ATP, at concentrations far above that necessary to saturate the high-affinity site on the enzyme, has regulatory effects on the Ca-ATPase. In one study, de Meis and Sorenson (1989) found that ATP, at concentrations greater than the level necessary to saturate the high-affinity site (10−400 μM), increases the rate of the E2 to E1 transition by binding to the E2 form of the enzyme. Lacapere et al. (1990) found that [ATP] between 1 and 100 μM enhance's changes in the intrinsic tryptophan fluorescence of the Ca-ATPase, which are associated with the E2 to E1 transition. This study concluded that [ATP] in this range exerted its effect by binding to the catalytic site of the Ca-ATPase in the E2 conformation (Lacapere et al., 1900). A recent study used intramolecular cross-linking by nucleotide analogs to demonstrate that the ATP binding site on the Ca-ATPase exists in two functional states, presumably the E1 and E2 conformations, since the presence of Ca distinguished between the two states (Gutowski-Eckel & Baumert, 1993).

Moller et al. (1980) compared ATP regulation in native SR to $C_{12}E_8$-solubilized Ca-ATPase, and found that in native SR ATP activated the Ca-ATPase in two phases. The first phase occurred from 2 to 50 μM ATP, and the second phase was only apparent above 100 μM ATP. Only the second phase of ATP activation was observed for solubilized Ca-ATPase; i.e., the solubilized enzyme was not activated below

100 μM ATP. The solubilized Ca-ATPase also had a lower affinity for ATP than the Ca-ATPase in native SR (Moller et al., 1980). The authors concluded that ATPase−ATPase interactions are essential for the modification of enzyme activity by ATP in the range of 10−100 μM (Moller et al., 1980), the same general range of [ATP] that accelerates the E2 to E1 transition, by ATP binding to the catalytic site in the E2 conformation (de Meis & Sorenson, 1989; Lacapere et al., 1990).

These studies provide insight toward understanding the mechanism of halothane and detergent effects on CPA inhibition of the Ca-ATPase. Seidler et al. (1989) determined that CPA does not interfere with FITC binding to the high-affinity site on the Ca-ATPase, and thus suggested that CPA did not interfere with high-affinity ATP binding to the Ca-ATPase. These results are consistent with our observations that CPA does not interact with the E1 conformation of the enzyme. Thus, CPA may interfere with ATP binding to the catalytic site in the E2 conformation, which has a lower affinity for ATP, and is responsible for accelerating the E2 to E1 transition. CPA may also interfere with the modulatory effects of ATP in the millimolar range, which are poorly understood. In the present study, we determined that $C_{12}E_8$ solubilization of the Ca-ATPase prevents ATP competition with CPA at [ATP] below 100 μM, and greatly increases the apparent K_I of CPA inhibition. Thus, CPA inhibition must be in part dependent upon ATPase−ATPase interactions. Since solubilizing the Ca-ATPase reduces the enzyme's affinity for ATP (Moller et al., 1980), it is reasonable to postulate that the affinity for CPA might also be reduced by solubilization, because they are competing for the same site on the enzyme. We conclude that halothane and $C_{12}E_8$ increase the apparent K_I of CPA inhibition by decreasing ATPase−ATPase interactions, which interferes with CPA binding at an ATP binding site in the E2 conformation.

Effects of Halothane and $C_{12}E_8$ on Phosphorylation from Inorganic Phosphate. CPA stabilizes and E2 form of the Ca-ATPase, which our phosphorylation results suggest is the E2 conformation of the Ca-ATPase rather than the E2−P conformation. CPA almost completely eliminated E−P formation, and reduced but did not completely eliminate E−P remaining when added after steady-state E−P levels had been reached (Figure 5). These two effects are both likely due to stabilization of the E2 conformation, as decay of E−P to nonzero levels under conditions which destabilize the E−P conformation has been observed previously (Froehlich & Heller, 1985). Halothane and $C_{12}E_8$ partially reversed the inhibitory effects of CPA on E2 phosphorylation from P_i (Figure 5). Addition of 7.6 mM halothane increased the apparent K_I of CPA inhibition by a factor of 4.8 (Figure 2), and increased the E2−P levels 4.5 times (Figure 5) over control (CPA alone). $C_{12}E_8$ solubilization of the Ca-ATPase increased the apparent K_I of CPA inhibition by a factor of 17 (Figure 3), and increased E2−P levels 17 times (Figure 5) over control (CPA alone). In a previous study, it was determined that incubation of the Ca-ATPase with 1 mM Ca prevents CPA-induced formation of enzyme oligomers (Mersol et al., 1993). This is consistent with our observation that CPA does not interact with the E1 conformation of the Ca-ATPase. These findings support a mechanism of CPA inhibition involving overstabilization of the E2 conformation which is in part dependent upon overstabilization of Ca-ATPase dimers or small oligomers.

Scheme 2: Model for CPA Inhibition of the Ca-ATPase in SR[a]

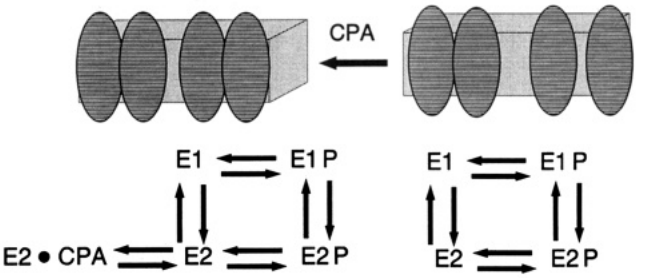

[a] In this model, CPA overstabilizes the E2 conformation in part by stabilizing small oligomers of the Ca-ATPase, preventing dynamic changes in the enzyme oligomeric state necessary for Ca-ATPase function.

It has previously been suggested that the Ca-ATPase enzymatic cycle (Scheme 1) involves a dimeric enzyme complex with coupled subunits, such that the E1 (or E1−P) to E2 (or E2−P) transition in one subunit is coupled to the E2 (or E2−P) to E1 (or E1−P) transition in the other subunit (Froehlich & Heller, 1985: Mahaney et al., 1994). We have shown that either over stabilizing Ca-ATPase oligomers with CPA or excessively depleting enzyme oligomers with halothane (Karon & Thomas, 1993) inhibits the enzyme. Thus, transient changes between the dimer and monomer states of the Ca-ATPase may be necessary to allow conformational changes in the coupled subunits. Though phosphorescence anisotropy experiments provide information on the Ca-ATPase oligomeric state only at equilibrium (because the enzyme is not cycling), other equilibrium measurements (such as FITC fluorescence and E−P formation) provide information on the biochemical action of CPA. Our results suggest that part of the mechanism of CPA-induced stabilization of the E2 conformation involves preventing transient dissociation of Ca-ATPase dimers that are necessary for conformational transitions of the enzyme (Scheme 2). In this case, we would expect that dissociating Ca-ATPase oligomers would destabilize the E2 conformation, and reduce the effectiveness of CPA in inhibiting enzymatic activity. These effects are observed when either halothane or $C_{12}E_8$ is added to SR in the presence of CPA.

Effects of Ca Loading on the Oligomeric State of the Ca-ATPase. Intravesicular Ca loading of SR has been reported to inhibit Ca-ATPase activity, and reduce the rate of E2 phosphorylation from inorganic phosphate (deMeis & Sorenson, 1989; Chaloub et al., 1979). Because CPA inhibits steady-state E2 phosphorylation from inorganic phosphate, and stabilizes small oligomers of the Ca-ATPase, we investigated the effects of Ca loading SR on the oligomeric state of the enzyme. Ca loading SR increased the fraction of immobile Ca-ATPase aggregates in SR, and sensitized SR to increased aggregation by CPA (Table 3). Because the experiments were performed at 4 °C to avoid Ca efflux from SR during the time course of the experiment, the predominant Ca-ATPase oligomers in the control (not Ca loaded, 4 °C) SR were tetramers and larger aggregates (Birmachu & Thomas, 1990). Thus, addition of CPA resulted in a change in the equilibrium between small oligomers (A_2), large oligomers (A_3), and immobile aggregates (A_∞'), rather than small oligomers (A_2) and monomers (A_1). The plant toxin thapsigargin, which inhibits the Ca-ATPase by stabilizing the E2 conformation, has also been shown to overstabilize Ca-ATPase dimers or small oligomers

(Sagara et al., 1992; Mersol et al., 1993). The effect of Ca loading of SR vesicles and thapsigargin on the oligomeric state of the Ca-ATPase is consistent with our proposal that the overstabilization of Ca-ATPase dimers or small oligomers under physiological conditions may play a role in overstabilization of the E2 conformation induced by SR perturbants.

Conclusion. CPA is a potent inhibitor of the Ca-ATPase in skeletal SR, and this inhibition is competitive with respect to ATP concentration. CPA inhibition of Ca-ATPase activity is dependent on the oligomeric state of the enzyme. Halothane and $C_{12}E_8$ protect the Ca-ATPase against CPA inhibition by decreasing the extent of ATPase interactions, thus increasing the apparent K_I of CPA inhibition. CPA stabilizes the E2 conformation of the Ca-ATPase relative to the E1 and E2−P conformations of the enzyme, and this effect is also dependent upon the extent of ATPase−ATPase interactions. We conclude that CPA inhibition is in part dependent upon CPA-induced stabilization of Ca-ATPase dimers or small oligomers. This physical effect is correlated with a CPA-induced stabilization of the E2 conformation of the Ca-ATPase, by competing with ATP for a binding site involved in the E2 to E1 transition.

ACKNOWLEDGMENT

We thank Razvan Cornea, Sandra Kaner, Howard Kutchai, and Joe Mersol for helpful discussions, and Robert Bennet, Nicole Cornea, John Matta, and Franz Nisswandt for technical support.

REFERENCES

Alonso, G. L., & Hecht, J. P. (1990) *J. Theor. Biol. 147*, 161−176.

Beeler, T., & Keffer, J. (1984) *Biochim. Biophys. Acta 773*, 99−105.

Bigelow, D. J., & Thomas, D. D. (1987) *J. Biol. Chem. 262*, 13449−13456.

Birmachu, W., & Thomas, D. D. (1990) *Biochemistry 29*, 3904−3914.

Birmachu, W., Nisswandt, F. L., & Thomas, D. D. (1989) *Biochemistry 28*, 3940−3947.

Birmachu, W., Voss, J. C., Louis, C. F., & Thomas, D. D. (1993) *Biochemistry 32*, 9445−9453.

Bishop, J. E., Squier, T. C, Bigelow, D. J., & Inesi, G. (1988) *Biochemistry 27*, 5233−5240.

Buhle, E. L., Knox, B. E., Serpersu, E., & Aebi, U. (1983) *J. Ultrastruct. Res. 85*, 186−203.

Chaloub, R. M., Guimaraes-Motta, H., Verjovski-Alameida, S., de Meis, L., & Inesi, G. (1979) *J. Biol. Chem. 254*, 9464−9468.

de Meis, L. (1988) *Methods Enzymol. 157*, 190−206.

de Meis, L., & Sorenson, M. M. (1989) *Biochim. Biophys. Acta 984*, 373−378.

Dupont, Y. (1980) *Eur. J. Biochem. 109*, 231−238.

Dux, L., Taylor, K. A., Ting-Beall, H. P., & Martonosi, A. (1985) *J. Biol. Chem. 260*, 11730−11743.

Eads, T. M., Thomas, D. D., & Austin, R. H. (1984) *J. Mol. Biol. 179*, 55−81.

Fernandez, J. L., Rosemblatt, M., & Hidalgo, C. (1980) *Biochim. Biophys. Acta 599*, 552−568.

Folch, J., Lees, M., & Sloane-Stanley, G. H. (1957) *J. Biol. Chem. 226*, 497−509.

Franzini-Armstrong, C., & Ferguson, D. G. (1985) *Biophys. J. 48*, 607−615.

Froehlich, J. P., & Heller, P. F. (1985) *Biochemistry 24*, 126−136.

Froud, R. J., & Lee, A. G. (1986) *Biochem. J. 237*, 197−206.

Gaffney, B. J. (1976) in *Spin Labeling Theory and Practice* (Berliner, L. G., Ed.) pp 567−571, Academic Press, New York.

Goeger, D. E., & Riley, R. T. (1989) *Biochem. Pharmacol. 38*, 3995−4003.

Gutowski-Eckel, Z., & Baumert, H. G. (1993) *Eur. J. Biochem. 218*, 823−828.

Hidalgo, C., Ikemoto, N., & Gergely, J. (1976) *J. Biol. Chem. 251*, 4224−4232.

Ikemoto, N., Garcia, A. M., Kurobe, Y., & Scott, T. L. (1981a) *J. Biol. Chem. 256*, 8593−8601.

Ikemoto, N., Miyao, A., & Kurobe, Y. (1981b) *J. Biol. Chem. 256*, 10809−10814.

Inesi, G. (1985) *Annu. Rev. Physiol. 47*, 573−601.

Kalabokis, V. N., Bozzola, J. J., Castellini, L., & Hardwicke, P. M. D. (1991) *J. Biol. Chem. 266*, 22044−22050.

Karon, B. S., & Thomas, D. D. (1993) *Biochemistry 32*, 7503−7511.

Kinosita, K., Ishiwata, S., Yoshimura, H., Asai, H., & Ikegami, A. (1984) *Biochemistry 23*, 5963−5975.

Lacapere, J., Bennet, N., Dupont, Y., & Guillain, F. (1990) *J. Biol. Chem. 265*, 348−353.

Louis, C. F., Zaulkernan, K., Roghair, T., & Mickelson, J. R. (1992) *Anesthesiology 77*, 114−125.

Ludescher, R. D., & Thomas, D. D. (1988) *Biochemistry 27*, 3343−3351.

Mahaney, J. E., & Thomas, D. D. (1991) *Biochemistry 30*, 7171−7180.

Mahaney, J. E., Froehlich, J. P., & Thomas, D. D. (1994) *Biophys. J. 66(2)*, A200.

Martonosi, A. N., Jona, I., Molnar, E., Seidler, N. W., Buchet, R., & Varga, S. (1990) *FEBS Lett. 268*, 365−370.

Mersol, J. V., Kutchai, H., Mahaney, J. E., & Thomas, D. D. (1993) *Biophys. J. 64(2)*, A306.

Moller, J. V., Lind, K. E., & Andersen, J. P. (1980) *J. Biol. Chem. 255*, 1912−1920.

Nelson, T. E., & Sweo, T. (1988) *Anesthesiology 69*, 571−577.

Saffman, P. J., & Delbrück, M. (1975) *Proc. Natl. Acad. Sci. U.S.A. 72*, 3111−3113.

Sagara, Y., Wade, J. B., & Inesi, G. (1992) *J. Biol. Chem. 267*, 1286−1292.

Seidler, N. W., Jona, I., Vegh, M., & Martonosi, A. (1989) *J. Biol. Chem. 264*, 17816−17823.

Squier, T. C., & Thomas, D. D. (1989) *Biophys. J. 56*, 735−748.

Squier, T. C., Hughes, S. E., & Thomas, D. D. (1988a) *J. Biol. Chem. 263*, 9162−9170.

Squier, T. C., Bigelow, D. J., & Thomas, D. D. (1988b) *J. Biol. Chem. 263*, 9178−9186.

Stephen, C. R., & Litle, D. M. (1961) *Halothane*, pp 1−14, Williams and Wilkins, Baltimore, MD.

Taylor, K. A., Dux, L., & Martonosi, A. (1986) *J. Mol. Biol. 187*, 417−427.

Thomas, D. D. (1986) in *Techniques for the Analysis of Membrane Proteins* (Ragan, C. I., & Cherry, R. J., Eds.) pp 377−431, Chapman and Hall, London.

Voss, J., Hussey, D., Birmachu, W., & Thomas, D. D. (1991) *Biochemistry 30*, 7498−7506.

Voss, J., Jones, L. R., & Thomas, D. D. (1994) *Biophys. J.* (in press).

Wakabayashi, S., Ogurusu, T., & Shigekawa, M. (1990) *Biochemistry 29*, 10613−10620.